



Synthesis of new Ni(II) complex of curcumin arginine ligand and evaluation of its antimicrobial potency

Dina S. Sheliel*, Usama El-Ayaan, Nagwa Nawar

Chemistry Department, Faculty of Science, Mansoura University, ET-35516-Mansoura, Egypt

* Corresponding author (D Sheliel; dinaelsayed@mans.edu.eg)

Received: 1/8/2021
Accepted: 9/8/2021

ABSTRACT: New $[\text{Ni}(\text{curarg})(\text{H}_2\text{O})_3] \cdot 5\text{H}_2\text{O}$ chelate of curcumin arginine Schiff base have been synthesized *via* template reaction. The structure of the new complex was fully elucidated by various techniques such as elemental (CHN) analyses, FT-IR and UV-visible spectroscopies. Moreover, molar conductance and magnetic measurements were also carried out. TG and DTG thermal measurements were performed. Thermodynamic and kinetic parameters of the studied complex were discussed utilizing Coats-Redfern and Horowitz-Metzger equations. Finally, the antimicrobial studies of the tested complex were also evaluated.

Keywords: Curcumin, arginine, thermal measurements, kinetic studies, antimicrobial activity

1. Introduction

Curcumin (or diferuloylmethane) is a yellow compound separated from the rhizomes of turmeric plant. The medicinal applications of curcumin have been reported since ancient times [1-5]. It has a wide range of numerous therapeutic activities such as antioxidant, anti-inflammatory [6-7] and anticancer [8-10]. Though, its clinical applications in antitumor therapy, curcumin has some limitations such as bioavailability, instability in a biological medium (poor stability *in-vivo*), susceptibility to oxidation, its rapid metabolism and low absorption [11-13]. Therefore, the researchers designed and synthesized several curcumin analogues through structural modifications to develop the bioavailability and anticancer potency of curcumin [14-15].

Complexation of amino acids with many metal ions play a vital role in different fields such as industry, pharmacy, and biology [16]. In this work, we used L-arginine as an amino acid due to its high biological study. L-arginine is considered an essential amino acid due to its physiologically strategic role in human body [17].

2. Experimental

2.1. Materials and reagents

All the materials used included curcumin, L-arginine (amino acid) and $\text{NiCl}_2 \cdot 6\text{H}_2\text{O}$. Furthermore, nitric acid (HNO_3), potassium hydroxide (KOH), and silver nitrate (AgNO_3) were purchased from sigma Aldrich. Organic solvents including absolute ethanol, dimethyl sulphoxide, were from Merck.

2.2. Characterization

Elemental analyses (C, H and N) data were determined *via* Perkin-Elmer 2400 series II analyzer. The contents of Ni(II) and Cl ions were estimated by volumetric and gravimetric analyses [18]. Sherwood magnetic susceptibility balance was utilized at room temperature to record the magnetic susceptibility of the paramagnetic complex. FT-IR spectroscopy were made by KBr discs in ($4000\text{-}400\text{ cm}^{-1}$) region on a Mattson 5000 FT-IR spectrophotometer. Moreover, Electronic spectra utilizing DMSO as a solvent were recorded at room temperature on a UV2 Unicam spectrophotometer. DTG-50 Shimadzu thermogravimetric analyzer was used for thermogravimetric analyses (TGA, DTG) from $20\text{ }^\circ\text{C}$ to $800\text{ }^\circ\text{C}$ with heating rate ($10\text{ }^\circ\text{C}/\text{min}$) and dynamic nitrogen atmosphere ($15\text{ mL}/\text{min}$). Finally, AJENCO, vision plus EC

3175 conductivity meter measured the molar conductance of 1×10^{-3} M of the prepared complex using DMSO as a solvent at room temperature.

2.3. In situ synthesis of Ni (II) complexes via template reaction

A 10 ml ethanolic solution of curcumin (1.0 mmol, 0.368 g) was added to a refluxing solution of L-arginine (1.0 mmol, 0.171 g) and KOH (1.0 mmol, 0.056 g) in distilled water (20 ml). A brick red color of the solution appeared immediately. Then the reaction mixture was refluxed for 3 h with constant stirring. A 5 ml solution of $\text{NiCl}_2 \cdot 6\text{H}_2\text{O}$ in distilled water was added to the reaction mixture. Then the reaction was refluxed with continuous stirring for another 2 h. The isolated solid complex was filtered off, washed thoroughly with hot ethanol and finally preserved in a vacuum desiccator over anhydrous calcium chloride. The yield of the separated complex was in high percentage (92%). The proposed structure of the studied complex is presented in **Fig. (1)**.

2.4. Antimicrobial activities

In vitro anti-microbial screening of the new complexes under investigations was tested according to the reported method [19] against different types of bacteria. The % A.I. was calculated by equation (1).

$$\% \text{ A. I.} = \frac{\text{inhibition Zone diameter of tested compound}}{\text{inhibition Zone diameter of standard}} \times 100$$

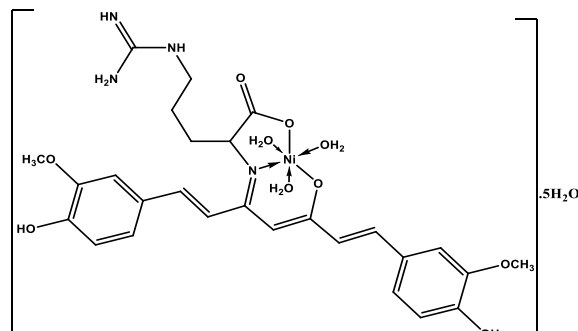


Fig. (1): The proposed structure of $[\text{Ni}(\text{curarg})(\text{H}_2\text{O})_3] \cdot 5\text{H}_2\text{O}$ complex.

3. Results and discussion

The Analytical and physical data of $[\text{Ni}(\text{curarg})(\text{H}_2\text{O})_3] \cdot 5\text{H}_2\text{O}$ complex is documented in **Table (1)**.

Table (1): The Analytical and physical data of $[\text{Ni}(\text{curarg})(\text{H}_2\text{O})_3] \cdot 5\text{H}_2\text{O}$ complex.

Complex (Empirical formula)	M.wt.; (g mol^{-1})	Color	M.P.; ($^{\circ}\text{C}$)	% Found (% Calcd.)				
				C	H	N	M	Cl
$[\text{Ni}(\text{curarg})(\text{H}_2\text{O})_3] \cdot 5\text{H}_2\text{O}$	725.37	Brownishorange	>300	44.23(44.71)	5.99(6.39)	7.11(7.72)	7.43(8.09)	-----

3.1. Molar conductance measurements

Molar conductance analysis is an important tool that affords effective information about the accurate structure of the complexes, the coordination number, and the nature of counter ions present inside or outside the coordination sphere in the synthesized complex. Therefore, it helps to sustain the electrolytic nature of the complex [20]. The molar conductance of $[\text{Ni}(\text{curarg})(\text{H}_2\text{O})_3] \cdot 5\text{H}_2\text{O}$ compound was measured at room temperature in DMSO (1×10^{-3} M). The low conductance value of Ni(II) complex which equals $5.55 \text{ Ohm}^{-1} \text{ cm}^2 \text{ mol}^{-1}$ purposed its non-electrolytic nature [21].

3.2. FT-IR spectroscopy

IR spectrum of $[\text{Ni}(\text{curarg})(\text{H}_2\text{O})_3] \cdot 5\text{H}_2\text{O}$ chelate as shown in **Fig. (2)**. demonstrates the new vibration band of coordinated nitrogen of azomethine group at 1622 cm^{-1} and coordinated (O-H) of water molecules at 3356 cm^{-1} . Two

new bands are observed in the regions 551 and 471 cm^{-1} attributable to Ni-O and Ni-N vibration bands, independently. Finally, the two bands of asymmetric and symmetric (COO^-) appears at 1586 cm^{-1} and 1418 cm^{-1} , respectively. The ligand acts as (NOO) bi-negative tridentate ligand around the Ni(II) ion.

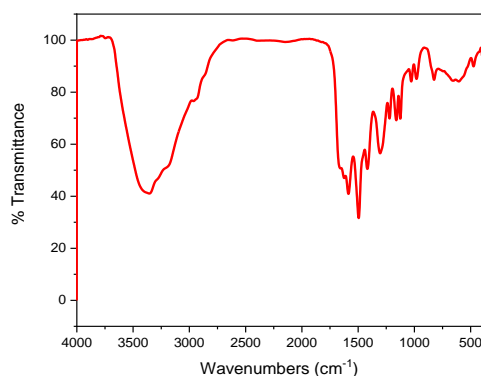


Fig. (2): IR spectrum of $[\text{Ni}(\text{curarg})(\text{H}_2\text{O})_3] \cdot 5\text{H}_2\text{O}$ complex.

3.3. UV-visible and magnetic moment studies

The electronic spectral bands of $[\text{Ni}(\text{curarg})(\text{H}_2\text{O})_3].5\text{H}_2\text{O}$ as appeared in **Fig. (3)** at 22271 and 23585 cm^{-1} may be due to ${}^3\text{A}_{2g} \rightarrow {}^3\text{T}_{1g}(\text{F})$ and ${}^3\text{A}_{2g} \rightarrow {}^3\text{T}_{1g}(\text{P})$ transitions, discretely. Also, the magnetic moment value equals (3.27 B.M) which proves its octahedral stereochemistry around Ni(II) ion [22].

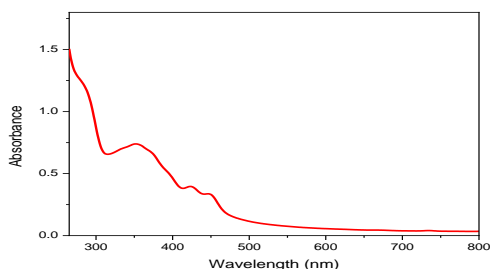


Fig. (3): Electronic absorption spectrum of $[\text{Ni}(\text{curarg})(\text{H}_2\text{O})_3].5\text{H}_2\text{O}$ complex.

Table (2): Decomposition steps within the temperature range ($^{\circ}\text{C}$) and weight loss for $[\text{Ni}(\text{curarg})(\text{H}_2\text{O})_3].5\text{H}_2\text{O}$ complex.

Compound	Temp. Range ($^{\circ}\text{C}$)	Removed species	Wt. Loss	
			% Found	% Calculated
$[\text{Ni}(\text{curarg})(\text{H}_2\text{O})_3].5\text{H}_2\text{O}$	26 - 141	$5\text{H}_2\text{O}$	11.991	12.414
	141 - 324	$3\text{H}_2\text{O} + 4\text{NH}_2 + \text{C}_{16}\text{H}_{17}\text{O}_4$	54.347	53.966
	324 - 426	$\text{C}_5\text{H}_5\text{O}_2$	13.362	13.385
	426 - 800	(Residue) $6\text{C} + \text{NiO}$	20.300	20.231

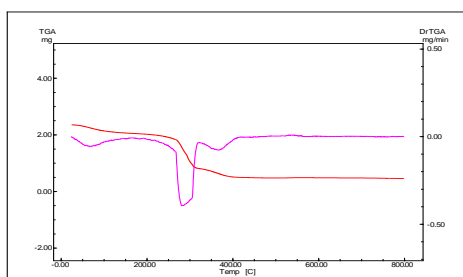


Fig. (4): TGA and DTG curves of $[\text{Ni}(\text{curarg})(\text{H}_2\text{O})_3].5\text{H}_2\text{O}$ complex.

3.5. Kinetic studies

Eyring equations [23-24] were applied to calculate the thermodynamic and kinetic

Table (3): Kinetic Parameters evaluated by Horowitz-Metzger and Coats-Redfern equations for $[\text{Ni}(\text{curarg})(\text{H}_2\text{O})_3].5\text{H}_2\text{O}$ complex.

Method	Peak	Mid Temp(K)	E_a KJ/mol	A (S^{-1})	ΔH^* KJ/mol	ΔS^* KJ/mol.K	ΔG^* KJ/mol
Coats-Redfern method	1 st	344.58	54.3824	1701891	51.51756	-126.832	95.22149
	2 nd	558.96	256.8118	1.03×10^{22}	252.1646	171.2922	156.4191
	3 rd	635.79	265.1322	5.98×10^{19}	259.8463	127.391	178.8523
Horowitz-Metzger method	1 st	344.58	60.32571	14339947	57.46087	-109.113	95.05895
	2 nd	558.96	261.396	4.62×10^{22}	256.7488	183.7405	154.0452
	3 rd	635.79	254.3759	1.24×10^{19}	249.0899	114.3005	176.4188

3.4. Thermal studies

The TG curve of $[\text{Ni}(\text{curarg})(\text{H}_2\text{O})_3].5\text{H}_2\text{O}$ **Fig. (4)** demonstrated four steps of thermal decomposition. As discussed in **Table (2)**, The first step in 26 - 141 $^{\circ}\text{C}$ range with a loss corresponding to $5\text{H}_2\text{O}$ molecules (water of crystallization) (Found: 11.991 %; Calcd.: 12.414 %). The second step lied in the range 141 - 324 $^{\circ}\text{C}$ and assigned to the loss of $3\text{H}_2\text{O}$ (coordinated water), 4NH_2 and $\text{C}_{16}\text{H}_{17}\text{O}_4$ fragment (Found: 54.347 %; Calcd.: 53.966 %). The third step occurred in the range 324 - 426 $^{\circ}\text{C}$ and attributed to the loss of $\text{C}_5\text{H}_5\text{O}_2$ fragment (Found: 13.362%; Calcd.: 13.385 %). Finally, the residual part in the temperature range 426-800 $^{\circ}\text{C}$ referred to $\text{NiO} + 6\text{C}$ in which the calculated loss was in match with the found loss (Found: 20.300 %; Calcd.: 20.231 %).

parameters. Data documented in **Table (3)** supposed that the decomposition stages are endothermic that was showed by the positive sign of ΔH^* value. Also, the majority of the degradation steps have a negative sign for entropies (ΔS^*) values indicating the well-ordered activated complex than the reactants. Finally, positive values of (ΔG^*) Gibbs free energy value clarify the non-spontaneous degradation stages. **Fig. (5)** and **Fig. (6)** display Coats- Redfern and Horowitz-Metzger plots for $[\text{Ni}(\text{curarg})(\text{H}_2\text{O})_3].5\text{H}_2\text{O}$ complex: (A) first, (B) second, and (C) third decomposition steps.

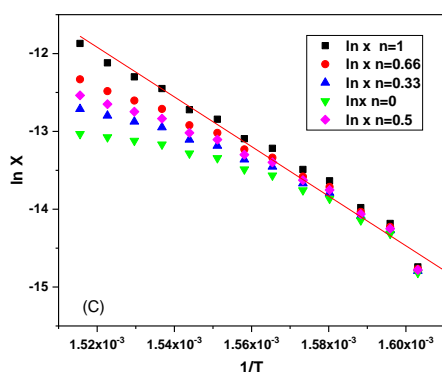
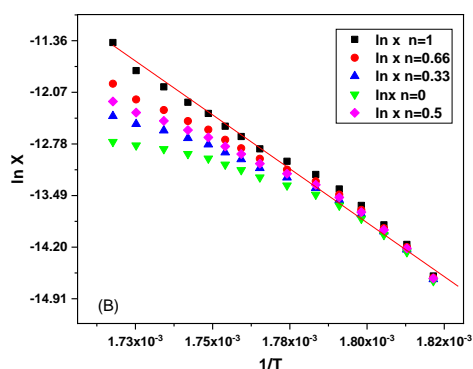
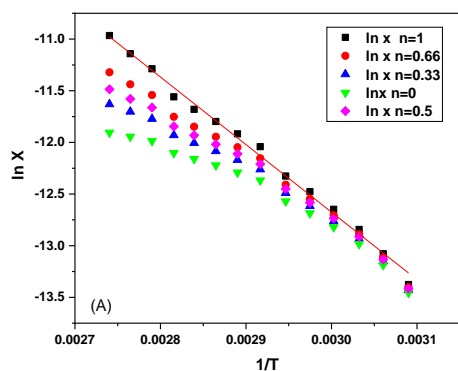


Fig. (5): Coats-Redfern plots for [Ni(curarg)(H₂O)₃].5H₂O complex: (A) first, (B) second, and (C) third decomposition steps.

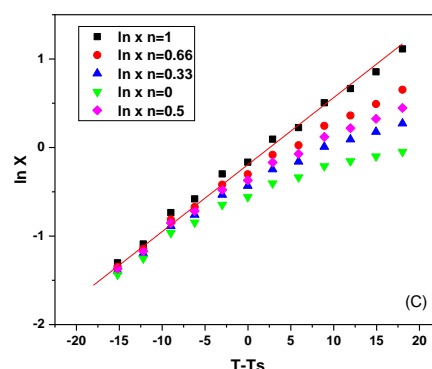
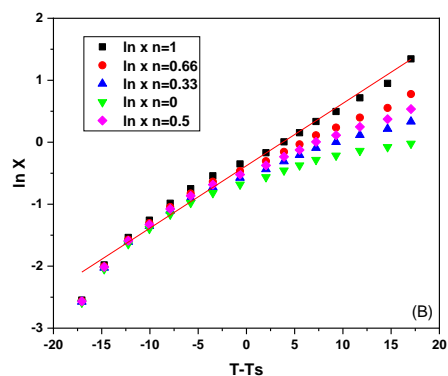
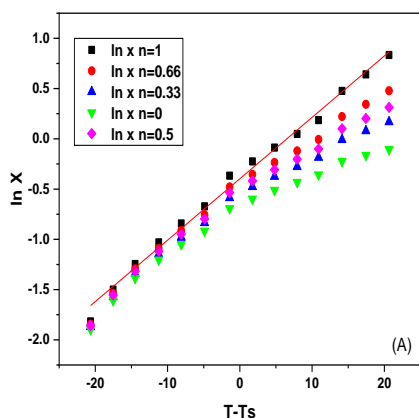


Fig. (6): Horowitz-Metzger plots for [Ni(curarg)(H₂O)₃].5H₂O complex: (A) first, (B) second, and (C) third decomposition steps.

3.6. Biological potency

3.6.1. Antimicrobial studies

In-vitro antimicrobial screening of the investigated [Ni(curarg)(H₂O)₃].5H₂O complex was inspected towards different types of bacteria: two-gram (+ve) bacteria such as *Bacillus subtilis* and *Staphylococcus aureus* in addition to two-gram(-ve) bacteria such as *Escherichia coli* and *Pseudomonas aeruginosa*. Ampicillin was used as a standard control in case of antibacterial activity. Moreover, their antifungal activity was investigated towards *Candida albicans* and Clotrimazole was used as a standard control in case of antifungal activity as presented in **Table (4)**. The following remarks were noticed from the experimental antimicrobial activities:

- 1- [Ni(curarg)(H₂O)₃].5H₂O showed no activity against *E. coli*.
- 2- In case of *Bacillus subtilis* the complex exhibited high anti-bacterial activity than the other bacteria.
- 3- In case of *C. Albicans* the complex exhibited moderate anti-fungal activity.

Table (4): Bacterial sensitivity (mm) of the $[\text{Ni}(\text{curarg})(\text{H}_2\text{O})_3].5\text{H}_2\text{O}$ complex against different bacterial and fungi strains

Compound	E. coli		Pseudomonas aeruginosa		S. aureus		Bacillus subtilis		C. Albicans	
	D (mm)	% A.I.	D (mm)	% A.I.	D (mm)	% A.I.	D (mm)	% A.I.	D (mm)	% A.I.
Ampicillin	24	100	23	100	23	100	25	100	NA	----
Clotrimazole	NA	----	NA	----	NA	----	NA	----	27	100
$[\text{Ni}(\text{curarg})(\text{H}_2\text{O})_3].5\text{H}_2\text{O}$	NA	----	3	13.0	5	21.7	8	32.0	10	37.0

Conclusion

In the present work, we isolated new Ni(II) complex derived from curcumin L-arginine Schiff base ligand. The results revealed that the new complex had octahedral geometry around Ni(II) ion. The infrared spectroscopy indicated that the ligand behaved as mononegative tridentate (NOO) around the metal center. The thermal studies showed the number of water molecules inside and outside the coordination sphere of the complex. The thermodynamic and kinetic parameters were estimated by Eyring equations. Finally, the antimicrobial activity of the complex was discussed.

References

- M.S. Refat, (2013) Synthesis and characterization of ligational behavior of curcumin drug towards some transition metal ions: Chelation effect on their thermal stability and biological activity, *Spectrochim. Acta, Part A* **105** 326-337.
- R. Motterlini, R. Foresti, R. Bassi, C.J. Green, (2000) Curcumin, an antioxidant and anti-inflammatory agent, induces heme oxygenase-1 and protects endothelial cells against oxidative stress, *Free Radic. Biol. Med.* **28 (8)** 1303-1312.
- C. Serpi, Z. Stanic, S. Girousi, (2010) Electroanalytical study of the interaction between dsDNA and curcumin in the presence of copper (II), *Talanta* **81 (4-5)** 1731-1734.
- P. Anand, A.B. Kunnumakkara, R.A. Newman, B.B. Aggarwal, (2007) Bioavailability of curcumin: problems and promises, *Mol. Pharmaceutics* **4 (6)** 807-818.
- B.B. Aggarwal, B. Sung, (2009) Pharmacological basis for the role of curcumin in chronic diseases: an age-old spice with modern targets, *Trends Pharmacol. Sci.* **30 (2)** 85-94.
- P. Jeyaraman, A. Alagarraj, R. Natarajan, (2019) In silico and in vitro studies of transition metal complexes derived from curcumin –isoniazid Schiff base, *J. Biomol. Struct. Dyn.*
- N. Shahabadi, M. Falsafi, N.H. Moghadam, (2013) DNA interaction studies of a novel Cu(II) complex as an intercalator containing curcumin and bathophenanthroline ligands, *J. Photochem. Photobiol. B Biol.* **122** 45-51.
- C. Sissi, F. Mancin, M. Gatos, M. Palumbo, P. Tecilla, U. Tonellato, (2005) Efficient plasmid DNA cleavage by a mononuclear copper(II) complex, *Inorg. Chem.* **44** 2310–2317.
- H.H. Tønnesen, J. Karlsen, A. Mostad, (1982). Structural Studies of Curcuminoids. I. The Crystal Structure of Curcumin. *Acta Chem. Scand. Ser. B*
- Y.M. Sun, H.Y. Zhang, D.Z. Chen, and C.B. Liu, (2002) Theoretical elucidation on the antioxidant mechanism of curcumin: a DFT study. *Organic letters*, 172909-2911.
- B.B. Aggarwal, A. Kumar, A.C. Bharti, (2003) Anticancer potential of curcumin: preclinical and clinical studies. *Anticancer research*, **23** 363-398.
- B.K. Adams, E.M. Ferstl, M.C. Davis, M. Herold, S. Kurtkaya, R.F. Camalier, M.G. Hollingshead, G. Kaur, E.A. Sausville, F.R. Rickles, J.P. Snyder, D.C. Liotta, M. Shoji, (2004) Synthesis and biological evaluation of novel curcumin analogs as anti-cancer and anti-angiogenesis agents, *Bioorg. Med. Chem.* **12** 3871-3883.
- T. Sarkar, S. Banerjee, S. Mukherjee, A. Hussain, (2016) Mitochondrial Selectivity and Remarkable Photocytotoxicity of a Ferrocenyl Neodymium(III) Complex of Terpyridine

- and Curcumin in Cancer Cells. *Dalton Trans.* **45** 6424-6438.
14. A. Valentini, F. Conforti, A. Crispini, A. De Martino, R. Condello, C. Stelitano, G. Rotilio, M. Ghedini, G. Federici, S. Bernardini et al. (2009) Synthesis, Oxidant Properties, and Antitumoral Effects of a Heteroleptic Palladium(II) Complex of Curcumin on Human Prostate Cancer Cells. *J. Med. Chem.* **52** 484-491.
 15. F. Caruso, M. Rossi, A. Benson, C. Opazo, D. Freedman, E. Monti, M.B. Gariboldi, J. Shaulky, F. Marchetti, R. Pettinari et al. (2012) Ruthenium–Arene Complexes of Curcumin: X-Ray and Density Functional Theory Structure, Synthesis, and Spectroscopic Characterization, in Vitro Antitumor Activity, and DNA Docking Studies of (*p*-Cymene)Ru(Curcuminato)Chloro. *J. Med. Chem.* **55** 1072-1081.
 16. S.E.H. Etaiw, D.M. Abd El-Aziz, E.H. Abd El-Zaher, E.A. Ali, Synthesis, spectral, (2011) antimicrobial and antitumor assessment of Schiff base derived from 2-aminobenzothiazole and its transition metal complexes, *Spectrochim. Acta A* **79** 1331-1337.
 17. M. Remko, D. Fitz, B.M. Rode, (2008) Effect of Metal Ions (Li^+ , Na^+ , K^+ , Mg^{2+} , Ca^{2+} , Ni^{2+} , Cu^{2+} , and Zn^{2+}) and Water Coordination on the Structure and Properties of L-Arginine and Zwitterionic L-Arginine, *J. Phys. Chem. A* **112**, 7652-7661.
 18. A.I. Vogel, Vogel's Textbook of quantitative chemical analysis, 5th ed., John Wiley & Sons, New work (1991).
 19. R.R. Zaky, T.A. Yousef, K.M. Ibrahim, (2012) Co (II), Cd (II), Hg (II) and U (VI) O₂ complexes of o-hydroxyacetophenone [N-(3-hydroxy-2-naphthoyl)] hydrazone: physicochemical study, thermal studies and antimicrobial activity, *Spectrochim. Acta A* **97** 683-694.
 20. R.G. Deghadi, W.H. Mahmoud, G.G. Mohamed, (2020) Metal complexes of tetradentate azo-dye ligand derived from 4, 4'-oxydianiline: Preparation, structural investigation, biological evaluation and MOE studies, *Appl. Organometal. Chem.* **34** (10) e5883.
 21. J.W. Geary, (1971) The use of conductivity measurements in organic solvents for the characterization of coordination compounds, *Chem. Coord. Rev.* **7** (1) 81-122.
 22. A.B.P. Lever, (1968). Inorganic electronic spectroscopy, *Studies in physical and theoretical chemistry* Elsevier, Amsterdam **33**
 23. A. Coats, J. Redfern, (1964) Kinetic parameters from thermogravimetric data, *Nature*, **201** (4914) 68-69.
 24. H.H. Horowitz, G. Metzger, (1963) A new analysis of thermogravimetric traces, *Anal. Chem.* **35** (10) 1464-1468.